Anal Bioanal Chem (2015) 407:6435–6445
DOI 10.1007/s00216-015-8806-z

RESEARCH PAPER

Electron microscopy of particles deposited in the lungs of nickel refinery workers

Miriam Küpper[1,2] · Stephan Weinbruch[1,2] · Vidar Skaug[2] · Asbjørn Skogstad[2] · Elín Einarsdóttir Thornér[2] · Nathalie Benker[1] · Martin Ebert[1] · Valery Chashchin[3] · Jon Øyvind Odland[4] · Yngvar Thomassen[2,5]

Received: 26 March 2015 / Revised: 22 May 2015 / Accepted: 26 May 2015 / Published online: 16 June 2015

Abstract The size, morphology, and chemical composition of particles deposited in the lungs of two nickel refinery workers were studied by scanning and transmission electron microscopy. The particles were extracted from the lung tissue by low-temperature ashing or by dissolution in tetramethylammonium hydroxide. The suitability of both sample preparation techniques was checked with reference materials. Both approaches lead to Fe-rich artifact particles. Low-temperature ashing leads to oxidation of small (diameter <2 μm) metallic Ni and Ni sulfide particles, dissolution in tetramethylammonium hydroxide to removal of sulfate surface layers. Silicates and alumosilicates are the most abundant particle groups in the lungs of both subjects. From the various metal-dominated particle groups, Ni-rich particles are most abundant followed by Fe-rich and Ti-rich particles. Ni appears to be present predominantly as an oxide. Pure Ni metal and Ni sulfides were not observed. The presence of soluble Ni phases was not investigated as they will not be preserved during sample preparation. Based on their spherical morphology, it is estimated that a large fraction of Ni-rich particles (50–60 % by number) as well as Fe-rich and Cu-rich particles (27–45 %) originate from high-temperature processes (smelting, welding). This fraction is much lower for silicates (3–5 %), alumosilicates (1–2 %), and Ti-rich particles (9–11 %). The absence of metallic Ni particles most likely results from low exposure to this species. The absence of Ni sulfides may be either ascribed to low exposure or to fast clearance.

Keywords Nickel refinery · Workplace aerosol · Electron microscopy · Lung deposition · Nickel species

Electronic supplementary material The online version of this article (doi:10.1007/s00216-015-8806-z) contains supplementary material, which is available to authorized users.

✉ Stephan Weinbruch
weinbruch@geo.tu-darmstadt.de

[1] Institute of Applied Geosciences, Technical University Darmstadt, Schnittspahnstr. 9, 64287 Darmstadt, Germany

[2] National Institute of Occupational Health, Gydas vei 8, PO Box 8149 Dep, 0033 Oslo, Norway

[3] Northwest Public Health Research Centre, 2-Sovetskaya 4, St. Petersburg 191036, Russia

[4] Department of Community Medicine, Faculty of Health Sciences, University of Tromsø—The Arctic University of Norway, Hansine Hansens veg 18, 9019 Tromsø, Norway

[5] Department of Plant and Environmental Sciences, Norwegian University of Life Sciences, 1432 Ås, Norway

Introduction

Inhalation is the main route of Ni exposure at workplaces. The most important health effects associated with occupational exposure to Ni are non-malignant respiratory diseases (asthma and fibrosis) and respiratory cancer (nasal and lung). Recent reviews on the toxicology of Ni are provided by Klein and Costa [1], the Nickel Institute [2], and Muñoz and Costa [3]. Solid Ni compounds that are of special concern are pure Ni metal, Ni alloys, oxidic Ni, sulfidic Ni, and soluble Ni (sulfate, chloride).

The exposure of workers in the Ni refinery at Monchegorsk (Kola Peninsula, Russia) has found considerable attention in the last 15 years [4–7], as it is the only refinery where a large number of women are employed, permitting epidemiological studies of reproductive effects [7–11]. Individual particle

analysis by scanning and transmission electron microscopy [5, 6] revealed a complex mixing state of the workplace aerosol particles in this Ni smelter. Almost all particles studied in the various departments of the refinery were heterogeneous on a nanometer scale [5, 6] and consisted of various Ni phases including metallic Ni, bunsenite NiO, trevorite $NiFe_2O_4$, heazlewoodite Ni_3S_2, godlevskite $(Ni,Cu)_9S_8$, orthorhombic $NiSO_4$, and an amorphous Ni, Cu, Al, Pb sulfate of variable composition [6].

In the present contribution, lung tissue samples from two workers employed in the smelter at Monchegorsk were investigated in order to study the fate of Ni-rich particles. It was reported earlier [12] that trevorite is the dominant, if not the only, Ni compound in the lungs of two workers employed in the Ni refinery at Kristiansand (Norway). This X-ray diffraction study [12] was limited to the magnetic fraction remaining after the lung tissue material was dry-ashed at 630 °C in a quartz crucible. In contrast, two sample preparation procedures (low-temperature ashing and dissolution in tetramethylammonium hydroxide) which preserve all solid Ni compounds except soluble Ni were applied in our study. Thus, it is expected to obtain more accurate information on the Ni phases contained in the lungs of refinery workers. In addition, the sample preparation techniques applied in the present contribution allow the study of other insoluble phases (e.g., silicates, Fe oxides) present in the lung tissue.

Experimental

Sample preparation

Preparation of lung tissue samples with low-temperature ashing

Frozen lung tissue samples were dried at approximately 50 °C for 24 h in a laboratory oven. Samples of 14.5 mg±0.5 mg (dry weight) were cut into small pieces (approximately 1 mm^3) in order to maximize the surface area (minimize the ashing time). The lung tissue samples were incinerated for 10 h with a TePla 100-E Plasma Processor instrument (PVA TePla AG, Feldkirchen, Germany) using 50 W forward power and an oxygen flow rate of 80 ml/min. The remaining ash was suspended in a mixture of 2–3 ml distilled water and some droplets of ethanol, and treated for 5 min in a Bandelin Sonorex RK 510 H ultrasonic bath (Bandelin GmbH, Berlin, Germany). Afterwards, approximately 200 μl of the suspension was applied on holey carbon TEM grids (Cu, 40 mesh, Agar Scientific, Stansted, UK). The remaining part of the suspension was filtered through polycarbonate filters (0.2 μm pore diameter, 25 mm diameter, Osmonics Inc., Minnetonka, USA). Areas of approximately 1 cm^2 of the filters were cut and attached on aluminum stubs with adhesive carbon pads. In total, 27 samples (including 3 blank samples) were ashed for SEM investigation. The blank samples were prepared by filtering a mixture of distilled water and some droplets of ethanol through a polycarbonate filter. The ashing time required to remove the lung tissue was determined by measuring the weight loss during incineration of dried lung tissue samples provided by the National Institute of Health (Oslo, Norway). After 10 h, no significant further decrease in mass was observed (Fig. 1). However, unashed pieces of lung tissue could still be observed by SEM, even after ashing for 14 h.

Preparation of lung tissue samples with tetramethylammonium hydroxide

Sample preparation followed procedures described in the literature [13]. Approximately 0.1 g of frozen lung tissue was mixed with 4 ml of distilled water and homogenized for 1 min using an Ultra-Turrax homogenizer (Typ TP 18.10, Janke & Kunkel KG, Staufen im Breisgau, Germany) operated at 20,000 rpm. The volume of the homogenized tissue was adjusted to 5 ml with distilled water, and 1 ml of this suspension was added to 3 ml 10 % tetramethylammonium hydroxide (TMAH) (Sigma-Aldrich Corporation, St. Louis, USA). After incubating for 30 min at room temperature, 10 ml of distilled water was added to each sample. Before filtering the samples through polycarbonate filters (0.2 μm pore diameter, 47 mm diameter, Osmonics Inc., Minnetonka, USA), they were incubated in a water bath at 65 °C for 25 min, being stirred every 5 min. After air-drying, approximately 1-cm^2 pieces were cut from the filters and attached to ethanol-cleaned aluminum stubs (12.5 mm diameter, Agar Scientific Limited, Stansted, UK) with adhesive pads. A piece of the remaining filter material of sample 1.3 TMAH (subject 1, peripheral area of the lower lobe, treated with TMAH; see Table 1) was wetted with ethanol and treated for 15 min in a Bandelin Sonorex TK 30 ultrasonic bath (Bandelin GmbH, Berlin, Germany). Afterwards, a drop of the suspension was applied on a holey carbon TEM grid (Cu, 40 mesh, Agar Scientific, Stansted, UK) and air-dried. Prior to filtration, approximately 40 μl of the suspension was separated and applied on ethanol-cleaned Si chips. In total, six samples (three samples on polycarbonate filters and three on Si chips) were prepared for SEM analysis.

Preparation of metallic Ni and Ni subsulfide samples

In order to check the oxidative influence of low-temperature ashing (LTA) and dissolution with TMAH on metallic and sulfidic Ni particles, pure metallic Ni powder (99.9 % Ni

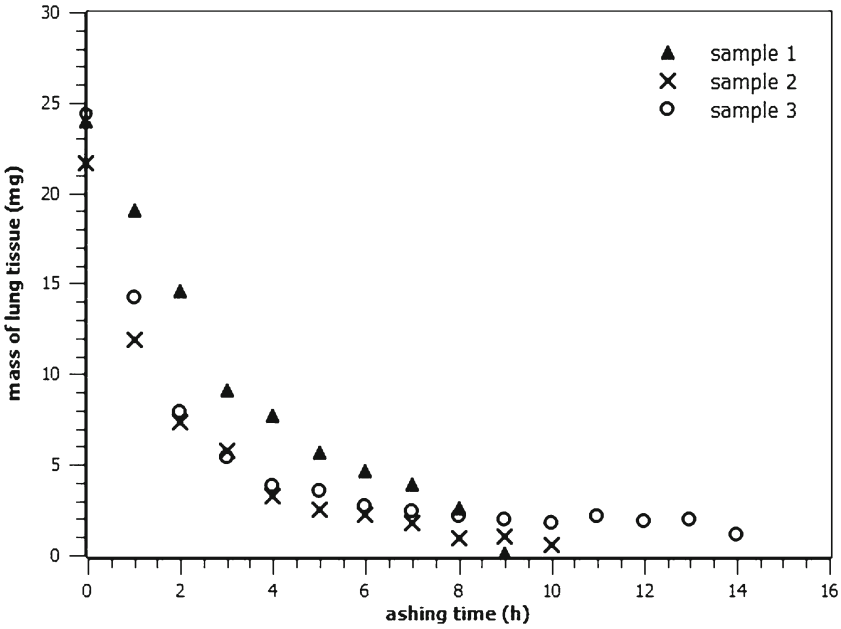

Fig. 1 Weight loss of three different lung tissue samples during low-temperature oxygen ashing (LTA)

metal, Alfa Aesar, Ward Hill, USA) and pure Ni subsulfide powder (α-Ni_3S_2, NIPERA, Durham, NC, USA) were investigated. The particles were applied in all experiments on silica chips to avoid a contribution of the substrate to the oxygen peak of the particles in the X-ray spectrum. Ni oxide particles were assumed to be stable under LTA as well as TMAH dissolution. Four different situations were investigated:

(a) Untreated samples of both materials were studied as reference.
(b) The influence of LTA was investigated by ashing the pure materials under similar conditions as the lung tissue samples.
(c) The influence of dissolution with TMAH was evaluated by suspending both materials in 10 % TMAH using the same treatment as during lung tissue sample preparation. Subsequently, the particles were spin-dried and washed in ethanol three times.
(d) In addition to the pure metallic Ni and α-Ni_3S_2 particles, mixtures of both materials with a pulverized lung tissue standard (Standard Reference Material 4351, National Institute of Standards, Gaithersburg, USA) were investigated.

Table 1 Lung regions the tissue samples were taken from

Sample identification	Lung region
1.1 and 2.1	Peripheral area of the upper lobe
1.2 and 2.2	Central area of the upper lobe
1.3 and 2.3	Peripheral area of the lower lobe
1.4 and 2.4	Central area of the lower lobe
1.11 and 2.11	Lymphatics at the trachea intersecting with the bronchus

Lung regions and subjects investigated

Frozen lung tissue samples were taken from different regions (Table 1) of the two subjects investigated. Except for the lymphatics sample, the tissue was taken from the left lung. Subject 1, male, was born in 1945. He was a smoker for 36 years and died from cardiovascular disease in 2000. Subject 2, male, was born in 1946. For a period of 30 years, he smoked 20 cigarettes per day. He suffered from chronic obstructive lung disease and died from cardiovascular disease in 2000. The work history of both individuals is summarized in Table 2.

Scanning electron microscopy

Scanning electron microscopy and energy-dispersive X-ray microanalysis (EDX) were carried out with two different instruments. Experimental parameters for automated analysis are given in the Electronic Supplementary Material (ESM) in Table S1. Automated analysis was restricted to particles with equivalent projected area diameters (d_p)≥0.05 μm. The obtained data set was checked manually, and substrate areas, which were erroneously declared as particles by the software, as well as particles with weak EDX signal were removed. In addition, artifact particles covering the filter surface of most of the samples prepared with LTA and occurring occasionally in

Table 2 Work history of the two subjects employed in the Ni refinery at Monchegorsk

Subject 1		Subject 2	
1967–1969	Welder	1970–1973	Tool shop worker (grinding and sharpening of blades containing hard metals)
1969–1991	Driver	1973–1988	Electroplating operator
1991–1992	Welder	1988–1998	Cutting and skinning of Ni sheets
1992–2000	Operator in Ni electrolyte purification department	Since 1998	Retired

the samples prepared with TMAH were also removed from the data set. Within the LTA samples, Fe-rich particles containing Ca, P, and Na were regarded as artifact particles in contrast to Fe-rich particles containing Cr, Mn, Ni, Cu, and Zn which were assumed to be inhaled particles. Due to these compositional differences, the latter can be easily recognized in backscattered electron images. In addition, most artifact particles in LTA samples have an irregular morphology differing significantly from the spherical and polygonal-shaped inhaled Fe-rich particles. The presence of such artifact particles in ashed lung tissue samples was described earlier [14]; they are assumed to stem from the lung tissue itself, originating from calcifications or from hemoglobin in the lung parenchyma [15]. Within the TMAH samples, agglomerates comprised of nanometer-sized primary particles containing Fe only were considered as artifact particles. These particles are presumably formed from hemoglobin in the tissue that was dissolved by TMAH and later resulted in the precipitation of Fe-rich particles [16]. Alternatively, they could have formed from Fe leached out of inhaled particles (e.g., from welding fume). However, as these particles are not deposited directly in the lung, they are still regarded as artifacts.

The X-ray count rates were corrected for matrix effects using the ZAF algorithm [17]. Geometric effects [18] were not corrected for. Based on their ZAF-corrected chemical composition (in wt%), the particles were classified into the following eight chemical groups: alumosilicates, silicates, (Ni-Fe-Cu-Ti) oxide/silicate mixtures, other metal/metal oxide mixtures, Ti oxide/silicate mixtures, Fe metal/metal oxide/silicate mixtures, Cu-oxide/silicate mixtures, and Ni oxide/silicate mixtures. The classification is first based on the element with the highest concentration out of Al, Si, Sn, Ti, Ce, V, Cr, Mn, Fe, Co, Ni, Cu, W, Zn, and Pb. In addition, all other elements occurring at high concentrations (i.e., above the concentration of the most abundant element minus 2 wt%) were also taken into account. The classification criteria are given in the ESM (Table S2).

Due to the large contrast difference in backscattered electron (BSE) images, particles with high metal concentrations and silicates/alumosilicates had to be analyzed in two different runs. Usually, the number of analyzed fields (i.e., analyzed area) in the two corresponding analyses was not identical. Therefore, the number of fields analyzed in the silicate/alumosilicate runs was normalized to the number of fields measured in the corresponding analyses of metal-rich particles of the same sample.

The particles were also classified according to their morphology into spherical particles, non-spherical particles, and agglomerates (Table 3). The spherical particles are assumed to originate from high-temperature processes (e.g., smelting, welding). Some of the non-spherically shaped particles have morphologies (e.g., elongated droplets) indicating that they originate from high-temperature processes as well.

Transmission electron microscopy and focussed ion beam investigations

Transmission electron microscopy was performed with a Philips CM 20 instrument (Philips, Eindhoven, The Netherlands) equipped with a Ge detector (Thermo NORAN, Middleton, USA) for energy-dispersive X-ray microanalysis (EDX). The instrument was operated at an acceleration voltage of 200 kV. The Ge detector enabled analysis of all elements with $Z \geq 6$ (carbon). A few spherical Ni oxide particles were sectioned with a focussed ion beam (FIB) using a Dual-beam Nova NanoLab 600 instrument (FEI, Eindhoven, The Netherlands).

Results

Development of sample preparation procedures

Three out of the four classes of solid Ni compounds defined by the International Committee on Nickel Carcinogenesis in Man [19] can be expected to be found as particles in lung tissue samples from employees in the Ni-producing industry: sulfidic, oxidic, and metallic Ni. Water-soluble Ni compounds (e.g., sulfates, chlorides) are not regarded here, as they will be most likely dissolved in the human respiratory tract quickly (see also "Particles deposited in the lungs"). Ni oxides are the most stable compounds and can be assumed to be stable

Table 3 Relative abundance [%] of different particle morphologies

Particle group	Relative abundance [%]			Number
	Spherical	Non-spherical	Agglomerates	
Subject 1				
(Ni, Fe, Cu, Ti) oxide/silicate mixtures	41.8	46.8	11.4	79
Other metal/metal oxide/ silicate mixtures	26.2	61.5	12.3	122
Ti oxide/silicate mixtures	11.4	64.9	23.7	561
Fe metal/metal oxide/ silicate mixtures	42.3	48.3	9.4	690
Cu oxide/silicate mixtures	45.7	28.6	25.7	35
Ni oxide/silicate mixtures	60.4	29.1	10.5	1189
Alumosilicates	1.4	97.5	1.1	1180
Silicates	5.4	93.5	1.1	926
Subject 2				
(Ni, Fe, Cu, Ti) oxide/silicate mixtures	28.3	54.6	17.2	99
Other metal/metal oxide/ silicate mixtures	12.3	57.5	30.1	73
Ti oxide/silicate mixtures	8.7	66.1	25.2	286
Fe metal/metal oxide/ silicate mixtures	27.3	49.0	23.7	304
Cu oxide/silicate mixtures	28.0	40.0	32.0	25
Ni oxide/silicate mixtures	50.3	33.1	16.6	850
Alumosilicates	1.4	98.0	0.6	307
Silicates	2.9	97.1	0.0	378

during LTA and dissolution with TMAH. Thus, the potential oxidation of metallic Ni and Ni subsulfide (α-Ni_3S_2) during sample preparation (LTA and dissolution in TMAH) was investigated.

Changes during low-temperature ashing

The results of ashing experiments are shown in the ESM separately for metallic Ni (Fig. S1a) and Ni subsulfide (Fig. S1b). For untreated metallic Ni particles, the O/Ni ratio remains approximately constant above a diameter of about 2 μm. A slight increase in the O/Ni ratio is observed for smaller grains, which may be explained by the presence of thin oxide layers already on the untreated particles. LTA for 10 h leads to a significant increase in the O/Ni ratio for small particles (d_p< 3 μm), indicating partial oxidation. If the metal particles are mixed with pulverized lung tissue standard and ashed, a large increase in the O/Ni ratio is observed, which most likely results from a contribution of the lung tissue material to the oxygen X-ray peak. Oxidation of Ni subsulfide particles (ESM Fig. S1b) during LTA is less pronounced than for the metallic Ni particles, as the O/(S+Ni) ratio is not significantly higher for ashed compared to untreated particles. The increase of the O/(S+Ni) ratio for particles with diameters below 2 μm in the untreated sample most likely indicates the presence of sulfates at the particle surface. As for metallic Ni, mixing Ni subsulfide particles with lung tissue standard prior to ashing leads to a strong increase of the oxygen X-ray peak.

Changes during treatment with tetramethylammonium hydroxide

The results of TMAH experiments are shown in the ESM (Fig. S2). As for LTA, the O/Ni ratio of untreated metallic Ni particles remains approximately constant for larger diameters (d_p>≈3 μm). For smaller particles, a slight increase of the O/Ni ratio is observed, most probably due to the presence of thin oxide layers. Treatment with TMAH for ½h does not lead to a significant change of the O/Ni ratio (ESM Fig. S2a). For Ni subsulfide, a completely different result is obtained (ESM Fig. S2b). The O/(S+Ni) ratio of particles suspended in TMAH for ½h is approximately constant over the whole size range. For small particles with diameters below 2 μm, the O/(S+Ni) ratio is smaller than for the untreated particles, and it is concluded that TMAH has dissolved the oxidized surface layers (consisting of sulfates) of the particles.

Inorganic particles deposited in the lungs

The size distribution (equivalent projected area diameter) of the particles encountered in the lung tissue samples is shown in Fig. 2, separately for silicates/alumosilicates and metal-rich particles, because the latter have a significantly higher density than silicates. It is remarkable that a higher abundance of large particles (silicates/alumosilicates as well as metal-rich particles) is observed in the lung region compared to the tracheobronchial region of subject 1 (Fig. 2).

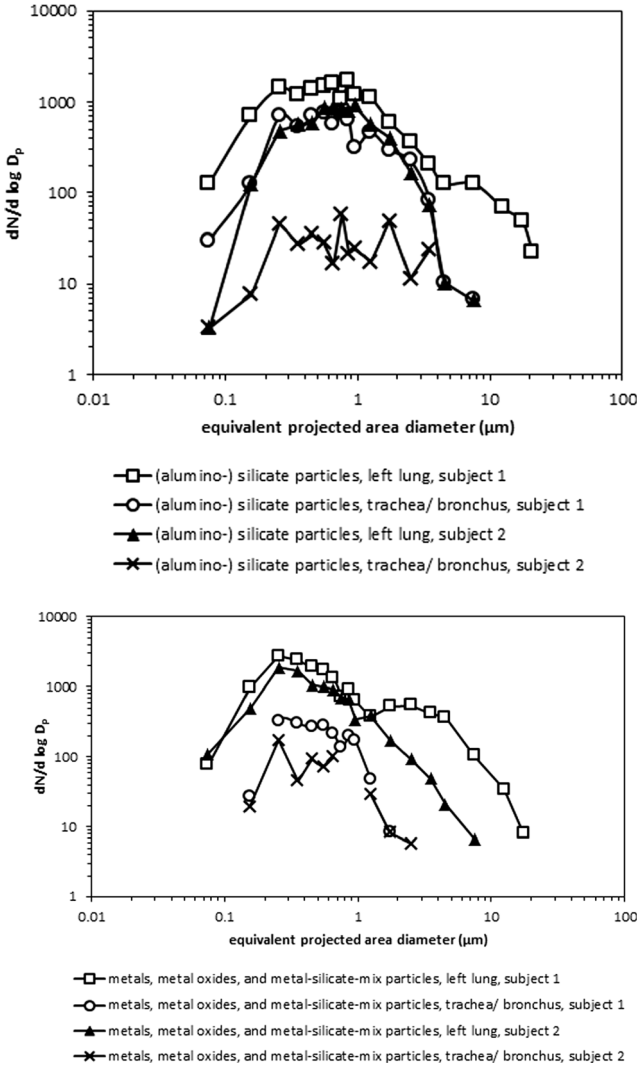

Fig. 2 Size distribution of silicates/alumosilicates (*upper part*) and metal-rich particles (*lower part*) deposited in the lungs of both subjects

The relative number abundance of the different particle groups observed in the LTA samples is shown in Fig. 3 for the different lung regions and the two subjects. For subject 1, silicate and alumosilicates are the dominating particle groups comprising about 80–97 % of all particles. For subject 2, the abundance of silicates and alumosilicates is significantly lower with a relative number abundance between 30 and 80 % (Fig. 3). For both subjects, the highest relative abundance of silicates and alumosilicates is observed in the tracheobronchial region (samples LTA 1.11 and LTA 2.11). From the various metal-dominated particle groups, Ni-rich particles are the most abundant group followed by Fe-rich particles. In both subjects, a high abundance of Ti-rich particles was observed in the tracheobronchial region. It is striking that no sulfide and only few pure metal particles are encountered within the metal-rich particle groups. Most particles within these groups appear to be oxides or mixtures of oxides with silicates. It may

Fig. 3 Relative number abundance of the different particle groups for subject 1 (**a**) and subject 2 (**b**) obtained from LTA. All particle groups are shown on the *left side*, only metal-rich groups on the *right side*

be suspected that the absence of pure metal particles is an artifact of our sample preparation, as mixing of metallic Ni particles with lung tissue prior to LTA led to a strong increase of the O/Ni ratio for particles with diameters below approximately 4 µm (ESM Fig. S1), indicating a contribution of unashed tissue material or the filter substrate to the X-ray spectrum of the particles. However, in the lung tissue samples of the two subjects investigated, pure Ni particles were not observed among the larger particles, where a contribution of unashed lung tissue or the filter substrate can be excluded. In addition, TEM did not yield any indication of the presence of metallic Ni particles (see below). Thus, it is concluded that pure Ni particles do not occur in the lung tissue of both subjects.

In order to check for a potential oxidation of metal and sulfide particles during low-temperature ashing, three lung tissue samples were prepared by dissolution in TMAH. The relative abundance of the different particle groups in these samples is shown in Fig. 4. Although the relative abundances obtained by dissolution in TMAH differ somewhat from those from LTA, it is confirmed that no sulfide and only few pure metal particles are present. The differences in the relative abundances between the LTA and TMAH samples are most likely due to statistical reasons (e.g., the smaller number of particles investigated in the TMAH samples).

The relative abundance of different particle morphologies is summarized in Table 3. It is differentiated between individual spherical particles (originating from high-temperature processes), individual non-spherical particles, and agglomerates (consisting of more than one primary particle).

Twenty-one Ni-rich particles from samples prepared by LTA were investigated by TEM. All particles were covered by a thin film (Fig. 5) consisting of carbon, phosphorous, and oxygen, and containing nanometer-sized (≤5 nm) heterogeneous inclusions of Fe and Sn particles. The Ni-rich particles generally contain only small amounts of Fe. It even cannot be excluded that the Fe signal originates from the nanometer-sized Fe inclusions within the surface film. Due to the surface film, it was not possible to obtain electron diffraction patterns or high-resolution images of the Ni-rich particles. One exemption was a particle of bunsenite (NiO).

Six spherical Ni-rich particles were sectioned with a focussed ion beam and then investigated by SEM and EDX. Five particles were chemically homogeneous and contained no core or inclusions of metallic Ni. One particle contained a heterogeneous inclusion that was too small to be characterized by energy-dispersive X-ray microanalysis.

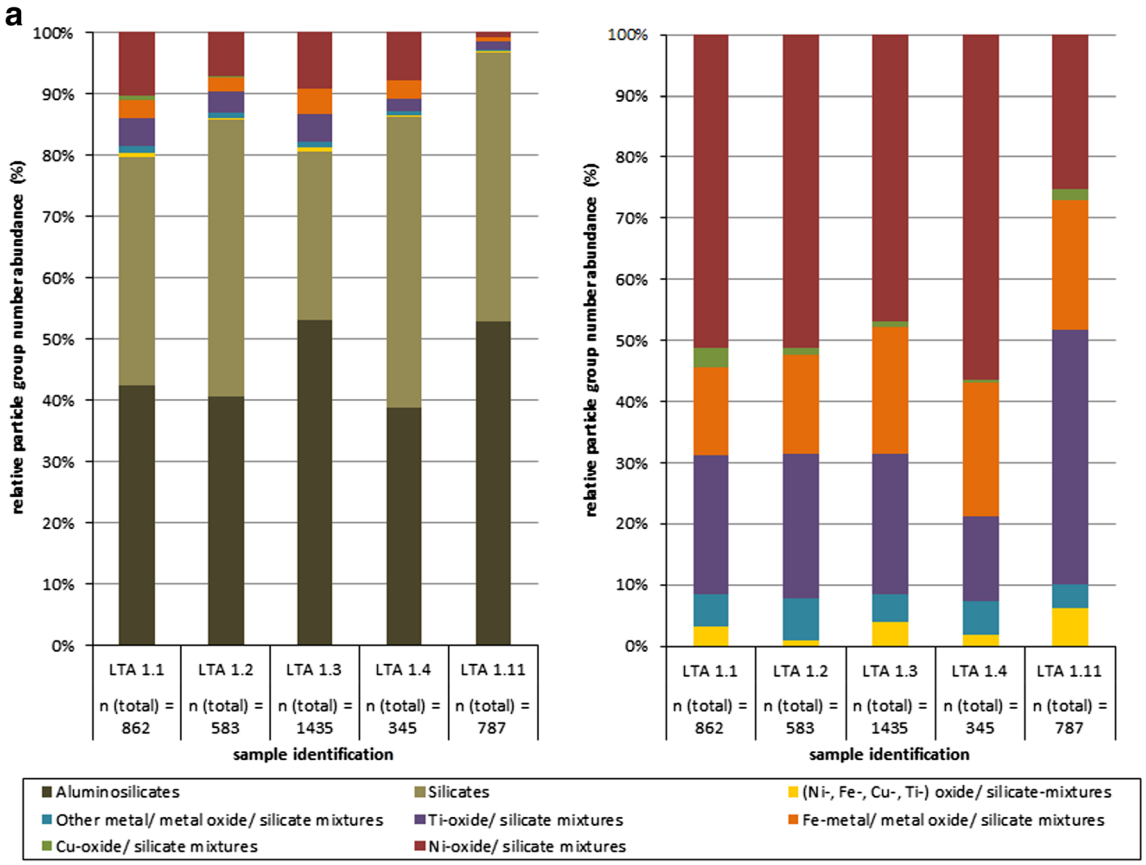
a
relative particle group numberabundance (%)
100%
90%
80%
70%
60%
50%
40%
30%
20%
10%
0%
LTA 1.1 n (total) = 862
LTA 1.2 n (total) = 583
LTA 1.3 n (total) = 1435
LTA 1.4 n (total) = 345
LTA 1.11 n (total) = 787
sample identification
Aluminosilicates
Silicates
(Ni-, Fe-, Cu-, Ti-) oxide/ silicate-mixtures
Other metal/ metal oxide/ silicate mixtures
Ti-oxide/ silicate mixtures
Fe-metal/ metal oxide/ silicate mixtures
Cu-oxide/ silicate mixtures
Ni-oxide/ silicate mixtures

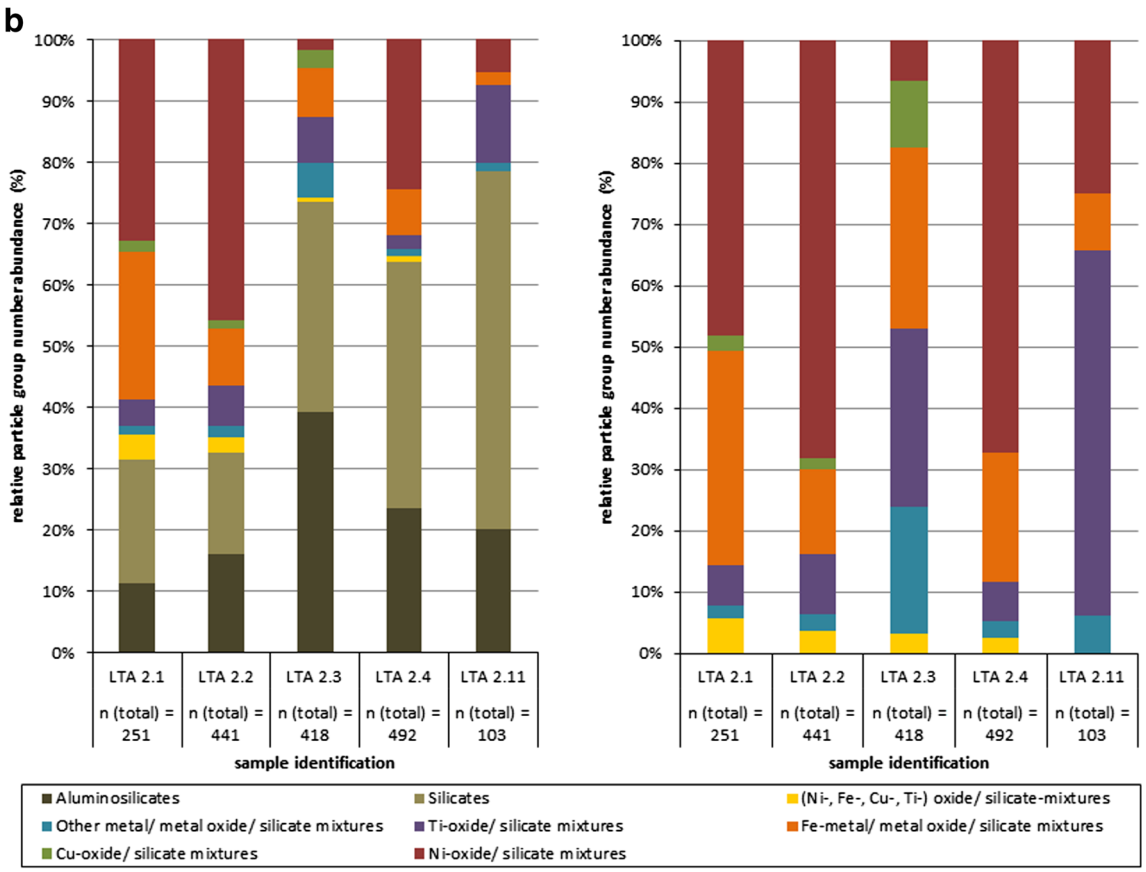
b
relative particle group numberabundance (%)
100%
90%
80%
70%
60%
50%
40%
30%
20%
10%
0%
LTA 2.1 n (total) = 251
LTA 2.2 n (total) = 441
LTA 2.3 n (total) = 418
LTA 2.4 n (total) = 492
LTA 2.11 n (total) = 103
sample identification
Aluminosilicates
Silicates
(Ni-, Fe-, Cu-, Ti-) oxide/ silicate-mixtures
Other metal/ metal oxide/ silicate mixtures
Ti-oxide/ silicate mixtures
Fe-metal/ metal oxide/ silicate mixtures
Cu-oxide/ silicate mixtures
Ni-oxide/ silicate mixtures

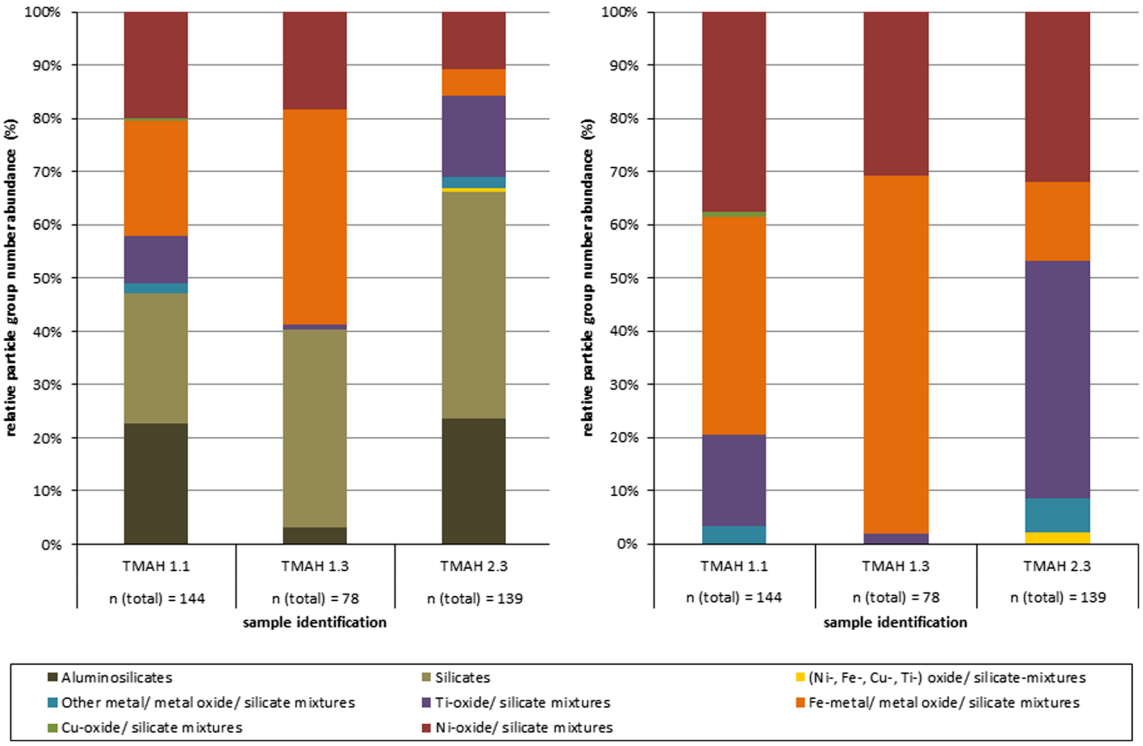

Fig. 4 Relative number abundance of the different particle groups within samples prepared by dissolution in TMAH (both subjects). All particle groups are shown on the *left side*, only metal-rich groups on the *right side*

Discussion

Comparison of sample preparation techniques

Both procedures (a comparison is given in Table 4) are generally well suited for preparation of particles from lung tissue samples, as they are cheap and have a high recovery. However, the occurrence of artifact particles has to be considered in both preparation techniques. During LTA, P-containing Fe oxide particles (sometimes also containing Na and Ca) are formed, which can be easily distinguished from other Fe oxides due to their characteristic chemical composition and morphology. After dissolution with TMAH, pure Fe oxide particles are encountered, which cannot be distinguished from Fe oxide particles deposited in the lung, neither by their chemical composition nor by their morphology (at least using automated analysis). However, as pure Fe oxide particles were not observed at workplaces in the smelter at Monchegorsk [5, 6], these particles are regarded as artifacts. During LTA, partial oxidation of metallic and sulfidic particles may occur. Dissolution with TMAH may result in removal of sulfate surface coatings (Table 4).

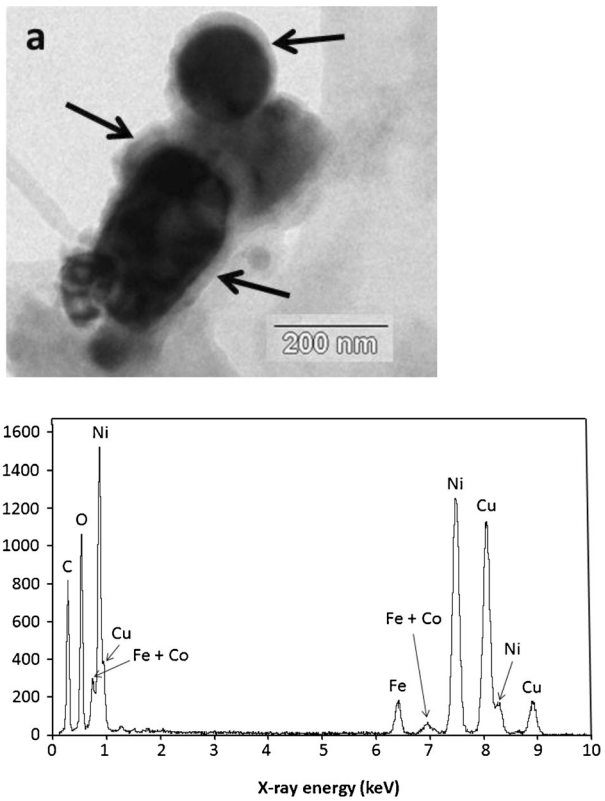

Fig. 5 TEM bright field image of Ni-rich particles (**a**) and corresponding X-ray spectrum (Cu peaks are an artifact from the TEM grid). The *arrows* in **a** denote the thin surface film observed on all particles studied by TEM

Particles deposited in the lungs

The most abundant particle groups encountered in the lung tissue of both subjects are silicates, alumosilicates, Ti oxide/

Table 4 Comparison of sample preparation procedures

Sample preparation	Low-temperature ashing	Dissolution in TMAH
Costs	Low	Low
Oxidation of metallic Ni	Yes (partially)	No
Oxidation of Ni sulfides	Yes (partially)	No
Dissolution of sulfate surface layer	No	Yes
Artifact particles	P-containing Fe-rich particles: easily recognized by typical morphology and chemical composition	Fe-rich particles: impossible to recognize from chemistry, difficult to recognize from morphology
Recovery	~85 % (Gylseth et al. 1981) [37]	~100 % (Murthy et al. 1973) [13]

silicate mixtures, Ni oxide/silicate mixtures, and Fe oxide/silicate mixtures (Fig. 3).

In both subjects, the highest relative number abundance is observed for silicates and alumosilicates. This is not surprising as both particle groups are major components of the particulate matter in ambient air. Most silicate and alumosilicate particles are non-spherical or agglomerates (93–95 %), indicating that the contribution of high-temperature processes (e.g., smelting, welding) is low. Still, a significant fraction of the silicate and alumosilicate particles may originate from occupational sources (e.g., ore processing).

The Ti oxide/silicate mixtures also seem to originate to a large extent from mechanical processes, as the fraction of spherical particles is low in both subjects (11.4 and 8.7 %). The exact contribution of occupational and environmental sources is not known. Titanium oxide particles may be emitted from different anthropogenic sources including metallurgy, pigment industries, coal burning, and welding [20–22]. As Ti oxides and Fe/Ti oxides are widespread minerals in the Monchegorsk region [23, 24], the non-spherical fraction (about 90 %) of Ti oxide/silicate mixtures may originate either from environmental sources or from occupational sources related to processing of the Ni ores in the smelter. In addition, some fraction of this particle group may be related to exposure to indoor air with Ti oxide pigments used in white paint as source.

Ni oxides/silicate mixtures originate to a large extent from smelting, as indicated by the high fraction of spherical particles (50–60 %) in both subjects. It is remarkable that practically all Ni-rich particles are Ni oxides. Ni sulfides were not observed; pure metallic Ni particles were (with the exception of one particle) also absent. However, it cannot be excluded that metallic Ni occurs as a minor constituent within the Ni-oxide/silicate mixtures although we have no indication of its presence.

Soluble Ni (i.e., sulfates or chlorides) was identified as the predominant component in the electrorefining and electrolyte purification departments in the Ni refinery in Monchegorsk [4, 25]. These particles are highly water soluble and undergo deliquescence instantaneously upon inhalation. More than 90 % of all particles present in the electrorefining department in Monchegorsk underwent deliquescence or developed a water film on the surface at a relative humidity of 96–98 % [25]. Thus, it can be assumed that these particles are already dissolved in the upper respiratory tract and that the soluble Ni fraction is excreted within a short period of time. Indeed, the half-life of Ni in rat lungs after inhalation was found to be about 32 h for Ni sulfate [26]. Furthermore, only 0.1 % of the dose was found in lung rats 21 days after tracheal instillation of Ni chloride [27]. In addition, soluble Ni particles left in the lungs of the workers would have been dissolved during sample preparation.

The absence of Ni sulfides may be ascribed to either a relatively low abundance in the workroom air or a short dissolution half time. The fraction of sulfidic Ni (relative to total Ni) was 3.7–7.7 % in the electrolyte purification department, with one exemption (19 %) below 2 % in the electrorefining department at Monchegorsk [4]. Similar low fractions of sulfidic Ni were observed within the electrolyte purification (1–3 %) and the electrorefining departments (5–6 %) of Scandinavian Ni refineries [28, 29]. Welding in the anode casting department at Monchegorsk was associated with even a lower (0.1 %) fraction of sulfidic Ni [4]. Alternatively, the absence of Ni sulfide particles may be explained by the short dissolution half time (T_{50}). For example, T_{50} in rat serum is 24 days for amorphous NiS and 34 days for α-Ni_3S_2 [30, 31]. The fast dissolution of Ni sulfates is in good agreement with the results of animal studies. The biological half time of Ni in the lungs of rats is 20 h for amorphous NiS [32], and 4.6 days for α-Ni_3S_2 [33].

The absence of metallic Ni most likely results from the low exposure to this Ni species. Subject 1 was employed in the last 8 years prior to his/her death as operator in the electrolyte purification department (Table 2). The fraction of metallic Ni (relative to total Ni) is <1–5.4 % in the electrolyte purification department at Monchegorsk [4]. Subject 2 was engaged in the

last decade prior to retirement with cutting and skinning of Ni sheets (Table 2), an occupation that is associated with exposure to metallic Ni [34]. However, the abundance of metallic Ni at this workplace in Monchegorsk is not known. The absence of metallic Ni particles in the lung tissue samples cannot be explained by a short dissolution half time. For example, the dissolution half time (T_{50}) of metallic Ni particles (median diameter<2 μm) in rat serum is >11 years [30]. In addition, the phagocytic index of metallic Ni was found to be much lower than for NiO [35]. Thus, it can be expected that oxidic Ni is cleared faster from the lungs than metallic Ni. As the metallic Ni particles were not oxidized during sample preparation with TMAH, their absence in the lung tissue cannot be explained by sample preparation (i.e., oxidation during LTA). Most particles encountered in the Ni refinery at Monchegorsk are complex mixtures of several phases [5, 6], and it could be suspected that metallic Ni particles are still present in the lung tissue samples and are included in agglomerates and/or may be partly oxidized (i.e., form the core of oxide particles). However, we do not have any indication from the chemical composition of the particles of such an occurrence of metallic Ni within our samples. In addition, we have sectioned six Ni oxide particles with a focussed ion beam and found no metal inclusions. In conclusion, the absence of metallic Ni particles in the lung tissue samples points to a low exposure to this Ni species.

Fe metal/metal oxide/silicate mixtures are also present at fairly high relative number concentrations up to 5 % in subject 1 and 20 % in subject 2 (LTA samples). A considerable fraction of these particles (42 % in subject 1 and 27 % in subject 2) has a spherical morphology indicating an origin from smelting processes or welding. The different Fe oxide phases cannot be determined with our experimental approach.

It was postulated earlier [12] that the Ni compound left in the lungs of workers some years after exposure is predominantly trevorite ($NiFe_2O_4$). Our investigations show that practically all Ni-dominated particles are Ni oxides with low Fe contents. Some of the Fe-dominated particles contain Ni amounts in accordance with the composition of trevorite. However, these particles are only a minor fraction of all Ni and Fe oxides observed in the present study. In addition to SEM where a large number of particles were studied, 21 Ni-rich particles were investigated in detail by TEM, and none of them had a composition in accordance with trevorite. Using the Wilson approximation for a binomial distribution [36], a 95 % confidence interval for the trevorite abundance of 0–15 % is obtained from the TEM data. The upper limit of approximately 15 % is in contradiction to the conclusion of Andersen and Svenes [12] that the dominating Ni phase left in the lungs is trevorite. The reasons for this discrepancy are not known.

Acknowledgments We would like to thank Gabriele Gorzawski for focussed ion beam investigations.

Ethical approval The manuscript was evaluated by the regional ethical committee of Norway (REK nord) at the University of Tromsø, and it was concluded by this committee that the study does not require an ethical approval.

Conflict of interest The authors declare that they have no competing interests.

References

1. Klein C, Costa M (2015) Nickel. In: Nordberg GF, Fowler BA, Nordberg M (eds) Handbook on the toxicology of metals, volume II, chapter 48, 4th edn. Elsevier, Amsterdam
2. Nickel Institute (2008) Safe use of nickel in the workplace, 3rd edn. Available at: www.nickelinstitute.org/NiPERA/WorkplaceGuide.aspx
3. Muñoz A, Costa M (2012) Elucidating the mechanisms of nickel compound uptake: a review of particulate and nano-nickel endocytosis and toxicity. Toxicol Appl Pharmacol 260:1–16
4. Thomassen Y, Nieboer E, Ellingsen D, Hetland S, Norseth T, Odland JO, Romanova N, Chernova S, Tchachtchine VP (1999) Characterisation of workers' exposure in a Russian nickel refinery. J Environ Monit 1:15–22
5. Höflich BLW, Wentzel M, Ortner HM, Weinbruch S, Skogstad A, Hetland S, Thomassen Y, Chaschin VP, Nieboer E (2000) Chemical composition of individual aerosol particles from working areas in a nickel refinery. J Environ Monit 2:213–217
6. Weinbruch S, van Aken P, Ebert M, Thomassen Y, Skogstad A, Chashchin VP, Nikonov A (2002) The heterogeneous composition of working place aerosols in a nickel refinery: a transmission and scanning electron microscope study. J Environ Monit 4:344–350
7. Vaktskjold A, Talykova LV, Chashchin VP, Nieboer E, Thomassen Y, Odland JO (2006) Genital malformations in newborns of female nickel-refinery workers. Scand J Work Environ Health 32:41–50
8. Chashschin VP, Artunina GP, Norseth T (1994) Congenital defects, abortion and other health effects in nickel refinery workers. Sci Total Environ 148:287–291
9. Vaktskjold A, Talykova LV, Chashchin VP, Odland JO, Nieboer E (2007) Small-for-gestational-age newborns of female refinery workers exposed to nickel. Int J Occup Med Environ Health 20:327–338
10. Vaktskjold A, Talykova LV, Chashchin VP, Odland JO, Nieboer E (2008) Spontaneous abortions among nickel-exposed female refinery workers. Int J Environ Health Res 18:99–115
11. Vaktskjold A, Talykova LV, Chashchin VP, Odland JO, Nieboer E (2008) Maternal nickel exposure and congenital musculoskeletal defects. Am J Ind Med 51:825–833
12. Andersen I, Svenes K (2003) X-ray diffraction spectrometric analysis of nickel refinery aerosols, process materials and particulates isolated from worker lung tissues. J Environ Monit 5:202–205
13. Murthy L, Menden EE, Eller PM, Petering HG (1973) Atomic absorption determination of zinc, copper, cadmium, and lead in tissues solubilized by aqueous tetramethylammonium hydroxide. Anal Biochem 53:365–372
14. Brody AR, Hill LH (1982) Interstitial accumulation of inhaled crysotile asbestos fibers and consequent formation of microcalcifications. Am J Pathol 109:107–114
15. Paoletti L, Batisti D, Caiazza S, Petrelli MG, Taggi F, de Zorzi L, Dina MA, Donelli G (1987) Mineral particles in the lungs of

subjects resident in the Rome area and not occupationally exposed to mineral dust. Environ Res 44:18–28
16. Krehula S, Musić S (2008) Influence of aging in an alkaline medium on the microstructural properties of α-FeOOH. J Cryst Growth 310:513–520
17. Goldstein J, Newbury D, Joy D, Lyman C, Echlin P, Lifshin E, Sawyer L, Michael J (2003) Scanning electron microscopy and x-ray microanalysis, 3rd edn. Springer, Heidelberg
18. Armststrong JT (1991) Quantitative elemental analysis of individual microparticles with electron beam instruments. In: Heinrich KFJ, Newbury DE (eds) Electron probe quantitation. Plenum Press, New York
19. Doll R (1990) Report of the International Committee on Nickel Carcinogenesis in Man. Scand J Work Environ Health 16:9–82
20. Ophus EM, Rode L, Gylseth B, Nicholson DG, Saeed K (1979) Analysis of titanium pigments in human lung tissue. Scand J Work Environ Health 5:290–296
21. Winchester JW (1984) Ambient aerosols in remote and polluted atmospheres. Nucl Inst Methods Phys Res B 3:454–461
22. Chen Y, Shah N, Huggins FE, Huffman GP (2005) Transmission electron microscopy investigation of ultrafine coal fly ash particles. Environ Sci Technol 39:1144–1151
23. Mitrofanov F (1995) Geology of the Kola Peninsula (Baltic Shield). Kola Science Centre, Apatity
24. Votekhovsky V, Pihlaja J (2011) Geochemistry in Khibiny mountains and Monchegorsk, Kola Peninsula, Russia (excursion guide, 25th International Applied Geochemistry Symposium 2011). Vuorimiesydistys – Finnish Association of Mining and Metallurgical Engineers, Rovaniemi
25. Inerle-Hof M, Weinbruch S, Ebert M, Thomassen Y (2007) The hygroscopic behaviour of individual aerosol particles in nickel refineries as investigated by environmental scanning electron microscopy. J Environ Monit 9:301–306
26. Hirano S, Shimada T, Osugi J, Kodama N, Suzuki KT (1994) Pulmonary clearance and inflammatory potency of intratracheally instilled or acutely inhaled nickel sulfate in rats. Arch Toxicol 68: 548–554
27. Carvalho SMM, Ziemer PL (1982) Distribution and clearance of ^{63}Ni administered as $^{63}NiCl_2$ in the rat: intratracheal study. Arch Environ Contam Toxicol 11:245–248
28. Werner MA, Thomassen Y, Hetland S, Norseth T, Berge SR, Vincent JH (1999) Correlation of urinary nickel excretion with observed 'total' and inhalable aerosol exposures of nickel refinery workers. J Environ Monit 1:557–562
29. Grimsrud TK, Berge SR, Resmann F, Norseth T, Andersen A (2000) Assessment of historical exposures in a nickel refinery in Norway. Scand J Work Environ Health 26:338–345
30. Kuehn K, Sunderman FW (1982) Dissolution half-times of nickel compounds in water, rat serum, and renal cytosol. J Inorg Biochem 17:29–39
31. Sunderman FW, Hopfer SM, Knight JA, McCully KS, Cecutti AG, Thornhill PG, Conway K, Miller C, Patierno SR, Costa M (1987) Physicochemical characteristics and biological effects of nickel oxides. Carcinogenesis 8:305–313
32. Tanaka I, Ishimatsu S, Haratake J, Horie A, Kodama Y (1988) Biological half-time in rats exposed to nickel monosulfide (amorphous) aerosol by inhalation. Biol Trace Elem Res 17:237–246
33. Benson JM, Henderson RF, McClellan RO, Hanson RL, Rebar AH (1986) Comparative acute toxicity of four nickel compounds to F344 rat lung. Fundam Appl Toxicol 7:340–347
34. Vincent JH, Ramachandran G, Kerr SM (2001) Particle size and chemical species "fingerprinting" of aerosols in primary nickel production industry workplaces. J Environ Monit 3: 565–574
35. Kuehn K, Fraser CB, Sunderman FW (1982) Phagocytosis of particulate nickel compounds by rat peritoneal macrophages in vitro. Carcinogenesis 3:321–326
36. Wilson EB (1927) Probable inference, the law of succession, and statistical inference. J Am Stat Assoc 22:209–212
37. Gylseth B, Baunan RH, Bruun R (1981) Analysis of inorganic fiber concentrations in biological samples by scanning electron microscopy. Scand J Work Environ Health 7:101–108